



Cite this: *Chem. Commun.*, 2014, 50, 13510

Received 31st July 2014,  
Accepted 8th September 2014

DOI: 10.1039/c4cc05990e

www.rsc.org/chemcomm

## Substrate-induced effects in thin films of a potential magnet composed of metal-free organic radicals deposited on Si(111)<sup>†</sup>

A. Caneschi<sup>a</sup> and M. B. Casu<sup>\*b</sup>

We deposit a paramagnetic pyrene derivative of the nitronyl nitroxide radical on Si(111). The molecules experience a strong chemical interaction with the substrate that influences the film growth. We also study the time evolution of the nitronyl nitroxide radical under a micro-focused soft X-ray beam, observing a stable radical as a product. This result hints at the possibility of using this class of materials in dosimeters and sensors.

The study of a variety of homo and heteroepitaxial growth processes involving metals and semiconductors has been successfully addressed with a wide range of experimental and theoretical tools developed in the last decades.<sup>1–4</sup> Since the seminal paper of Aviram and Ratner in 1974<sup>5</sup> molecules have also emerged as excellent candidates for applications in organic electronics. The understanding of systems, such as small organic molecules, colloids, organic-based magnets, all rapidly gaining attention due to their possible use in electronics, provides challenges that still need to be tackled. Indeed, the use of such new materials demands detailed knowledge of their growth mode, in order to optimize preparation conditions for applications. This is one of the focal points in molecular and organic magnetism.<sup>6,7</sup> In this respect, we have recently focused our efforts towards the comprehension of thin film processes (in the nanoscale regime) of open shell systems by investigating a pyrene derivative of the nitronyl nitroxide radical (4,4,5,5-tetramethyl-2-(pyrenyl)-imidazoline-1-oxy-3-oxide, NitPyn, Fig. 1) which has been deposited on a number of technologically relevant surfaces, namely silicon dioxide,<sup>8</sup> sapphire,<sup>9</sup> and titanium dioxide.<sup>10,11</sup>

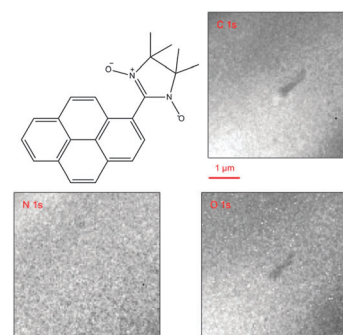


Fig. 1 NitPyn molecular structure. XPEEM images (photon energy: 600 eV) of a NitPyn film (nominal thickness 2.2 nm) deposited on Si(111)-7 × 7. The feature in the central part of the images is a surface defect; it was used to check the correctness of the microscope focus.

Our efforts are motivated by the immense technological potential of such materials, as they bring together magnetism and the flexibility of chemical synthesis.<sup>12–15</sup> In a previous X-ray photoelectron spectroscopy (XPS) and electron spin resonance (ESR) investigation, we demonstrated that NitPyn could be successfully evaporated without suffering from molecular degradation, while preserving its paramagnetic character.<sup>16</sup>

In this work, we use X-ray photoelectron emission microscopy (XPEEM) and related microprobe methods to investigate the morphology of thin films of NitPyn deposited on well characterized Si(111) surfaces; we focus in particular on the substrate–molecule interactions and their role in determining a homogeneous growth.

XPEEM with synchrotron radiation is a powerful microscopy technique that gives access to the lateral composition of organic interfaces. In combination with low energy electron microscopy, it offers the capability to correlate morphology, structure, and electronic properties.<sup>17–21</sup> Our investigations are carried out using a spectroscopic photoemission and low-energy electron microscope (SPELEEM), a set-up which allows combining imaging, diffraction, and microprobe-spectroscopy.<sup>18</sup> Microprobe-XPS is particularly useful due to the reduced acquisition times, which

<sup>a</sup> Department of Chemistry and RU INSTM, University of Florence, Via della Lastruccia 3, I-50019 Sesto Fiorentino, Italy

<sup>b</sup> Institute of Physical and Theoretical Chemistry, University of Tübingen, Auf der Morgenstelle 18, D-72076 Tübingen, Germany.  
E-mail: benedetta.casu@uni-tuebingen.de

<sup>†</sup> Electronic supplementary information (ESI) available: Experimental section. The overview XPS spectrum after NitPyn deposition. The table containing the NitPyn stoichiometry and integrated XPS experimental signal intensities for the thin films. The overview XPS spectrum after annealing at 570 K. XPS profiles extracted from the time-dependent C 1s signal. See DOI: 10.1039/c4cc05990e



is vital in providing information on the chemical bonding, without damaging the film. Fig. 1 shows C 1s, N 1s, and O 1s XPEEM images of a NitPyn thin film deposited on a Si(111) substrate. All XPEEM images are featureless within the lateral resolution of our instrument that is 50 nm for the conditions of the present experiments, revealing a homogenous lateral distribution of NitPyn on the Si(111)-7 × 7 substrate. This is a surprising result, since in previous experiments on NitPyn on different substrates (gold,<sup>16</sup> sapphire,<sup>9</sup> and titanium dioxide<sup>10,11</sup>), carried out using the same evaporation rate and substrate temperature adopted in this work, we obtained films characterized by strong 3D island formation.<sup>8,9,11,16</sup> To shed light on the XPEEM finding and investigate the electronic structure of the films, we exploit a specific operation mode that the SPELEEM microscope offers, namely microprobe spectroscopy, investigating the relevant core levels (N 1s, C 1s, O 1s, and Si 2p), and, thus, the chemical environment of the NitPyn molecules on Si(111). This operation mode permits fast acquisition times, minimizing radiation damage on the sample.

The results for the C 1s, N 1s, and the O 1s core levels are shown in Fig. 2, along with the fit of the spectra. The spectra show the expected features with the C 1s main line at around 285 eV. The N 1s and O 1s spectra are characterised by spectroscopic lines peaked at 398.5 eV and at 531.9 eV, respectively. The ratio of the integrated signal intensities of the different lines of the XPS curves indicates a slight overestimation of the nitrogen present in comparison with carbon concentration, possibly due to the fact that we do not take into account all C 1s satellite intensities<sup>22,23</sup> (the measured N/C ratio is 0.10 to be compared with 0.09, as expected on the basis of NitPyn stoichiometry, see the ESI† for details). A best fit procedure applied to the C 1s spectroscopic line is based on four single contributions,<sup>16</sup> and it nicely agrees with the stoichiometry values (see Fig. 2, and ESI†). These four nonequivalent C 1s core level contributions, expected due to the different atomic local chemical environments, are classified into two groups: the aromatic (C–C and C–H) and the methyl group (CH<sub>3</sub>) carbon sites contribute to the lower binding energy feature, while the shoulder at higher binding energies can be attributed to the signal from nitrogen-bonded carbon atoms.<sup>16</sup> For the sake of simplicity, we include the first shake-up satellite intensity in the main line intensity, according to ref. 16. The N 1s and O 1s core level spectra of an intact mesomeric nitronyl nitroxide

radical are characterized by a single peak.<sup>16</sup> They carry the information about the paramagnetic function of this pyrene derivative, since the unpaired electron is delocalized over the two equivalent NO groups. We note that the peak binding energy for the N 1s spectrum and the O 1s core level spectrum peak energies correlate very closely with the expected binding energy of photoelectrons emitted from nitrogen and oxygen atoms involved in a chemical bond with silicon,<sup>24–27</sup> as for example in silicon oxynitrides.<sup>25</sup> These values indicate a rather strong interaction of NitPyn molecules on the Si(111) substrate. The conclusion of a strong interaction between the molecules and the Si(111) substrate is also supported by the fact that the molecules still cover the surface after annealing the films at around 570 K, and the N/C ratio is preserved (see ESI†). For comparison, note that physisorbed NitPyn molecules on Au(111) single crystals desorb completely after annealing at 550 K,<sup>16</sup> and a similar behavior is observed in NitPyn on sapphire.<sup>9</sup> Consequently, these observations suggest that the nitronyl nitroxide radical interacts very strongly with the silicon substrate leading to chemisorption of NitPyn molecules. A strong substrate–molecule interaction is not unusual for molecules deposited on Si(111)-7 × 7 surfaces, and it may also hinder the azimuthal order of the adsorbate.<sup>24,28</sup> This also occurs in the present case, since we obtain featureless low energy electron diffraction patterns (not shown). Looking in detail at the N 1s spectroscopic line, and adopting a best fit procedure, we observe that the N 1s core level spectrum is characterized by two contributions. We assign the contribution at higher binding energy to the first shake-up satellite, because of its energy position with respect to the main line (the difference in energy is 1.5 eV). Shake-up satellites are characteristic features in photoemission core level spectra, due to electronic relaxation effects. The energy distance of the first shake-up satellite, *i.e.*, the HOMO–LUMO shake-up satellite, is lower than the molecular optical gap because of the enhanced screening of the core–hole due to its delocalization over the aromatic system.<sup>29</sup> This effect is typical for polyaromatic systems such as polyacenes<sup>29</sup> or perylene-based molecules.<sup>30</sup> The value of 1.5 eV is in good agreement with tetracene (1.48 eV),<sup>29</sup> and our previous work on NitPyn.<sup>8,9</sup> It is interesting to note that the contribution we assign to the HOMO–LUMO satellite is very intense. This further supports that a strong interaction between NitPyn and Si(111) exists.<sup>31</sup> Because of the fact that we observe this strong satellite in the N 1s core level spectra, we may infer that the strong interaction leads to a large redistribution of the electronic density in the radical upon core–hole creation. What is more important is the influence of the strong substrate–molecule interaction on the paramagnetic character of the NitPyn molecules on top of the silicon surface. The strong chemisorption perturbs the two NO groups and, consequently, we may assume that NitPyn paramagnetic character is perturbed by the chemical bond with silicon, as we observed for NitPyn at the interface with rutile TiO<sub>2</sub>(110) single crystals.<sup>10</sup>

The above observations, based on an accurate analysis of the chemical environment of the NitPyn molecules at the interface with the Si(111)-7 × 7 surface, are the key step to interpret the

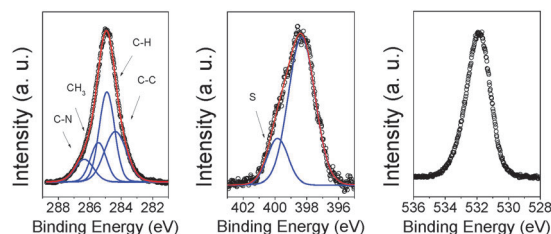
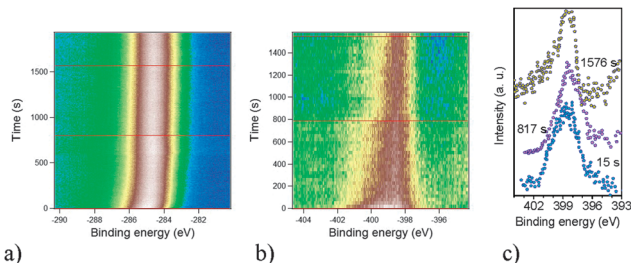


Fig. 2 C 1s, N 1s and O 1s core level photoemission spectra of NitPyn thin films deposited on Si(111)-7 × 7 at room temperature, together with their fit curves (see ESI† for fit details), as indicated. Photon energy: 600 eV. Cumulative acquisition time: max 120 s.





**Fig. 3** Time-dependent (a) C 1s and (b) N 1s signals. Color scale: green represents the background signal; white the initial peak intensity. (c) XPS profiles extracted from the time-dependent N 1s signal (see line profiles in b, the C 1s line profiles are shown in ESI<sup>†</sup>), for the beam exposure, as indicated. Photon energy: 600 eV.

absence of 3D islands on our samples. It is well-known that strong substrate–molecule interactions are also important in layer-by-layer growth: the molecules are more strongly bound to the substrate than to each other. The layer-by-layer mode will be sustained, providing a continuous decrease in bonding energy toward the bulk-crystal value.<sup>1,2</sup> In NitPyn deposited on Si(111), the layers, beyond the first one, do not chemically interact with the Si(111) surface. Nevertheless, the interaction with the substrate experienced by those layers is strong enough to favor the two-dimensional film morphology against island nucleation. We now consider the radiation sensitivity of our organic films. In order to evaluate the stability of the molecular film under an intense, microfocussed X-ray beam (flux of  $1 \times 10^{12}$  ph s<sup>-1</sup> over 70  $\mu\text{m}$  squared), the micro-XPS operation mode is used to monitor the time evolution of the C 1s, N 1s and O 1s core level emission. In this manner, we can quantify the degradation pattern and the fingerprint of radiation damage in real time. The results are shown in Fig. 3, where the C 1s and N 1s signals are plotted as a function of time. The initial N 1s signal is characterized by a main line peaked at 398.5 eV, as shown in Fig. 2. We observe a decrease in the peak intensity with time (see Fig. 3b, the peak maximum changes from white to brown in the color scale representation, and Fig. 3c), and a progressive shift of the peak towards lower binding energies, while the signal in the binding energy range below 396 eV starts to increase (Fig. 3c). After 800 s of beam exposure, the N 1s spectroscopic line experiences a clear narrowing and a signal appears in the lower binding energy range (Fig. 3b and c). Breaking the nitrogen bond with oxygen hinders the electron withdrawing action of the oxygen atoms, pushing down the binding energy of the electrons emitted from the derivatives with respect to the signal of the intact molecules. Therefore, a similar photo-induced reaction pathway can be the reason for the line narrowing and the signal appearing for binding energies below 396 eV: under the photon beam, the nitronyl nitroxide radical releases an oxygen atom becoming an imino nitroxide radical. The interesting result is that the pyrene substituent stays intact (see Fig. 3a and Fig. 3S in ESI<sup>†</sup>), the change is experienced only by the nitronyl nitroxide part of the molecule and it is possible to identify the resulting radicals (imino nitroxide) by using XPS, as in this work, or *ex situ* by ESR.<sup>8,16,32,33</sup> This is in good agreement with the characterisation of nitronyl nitroxide

radical derivatives in solution: they show the tendency to spontaneously lose an oxygen atom, without further decomposition.<sup>32</sup> The compounds are stable and can be reconverted to the initial one with an appropriate acid treatment.<sup>32</sup> Therefore, developing an analogous controlled reversible degradation in NitPyn thin films will certainly pave the way for their technological use.

In conclusion, we present a photoelectron emission microscopy investigation of the composition and stability of a potential metal-free magnet based on a pyrene derivative of the nitronyl nitroxide radical deposited on the Si(111)-7  $\times$  7 surface. The strong interaction between the molecules and the surface influences not only the electronic structure of the molecule at the interface, but our results also suggest that the strong molecule–substrate interaction influences the growth mode of the thin films, favoring a homogeneous film texture. We also investigated in real time the radiation sensitivity of NitPyn films. The observed degradation pattern, if successfully controlled and reproduced, can be exploited for its technological use in dosimeters and sensors.

The authors thank Elettra-Sincrotrone Trieste for providing beamtime, Onur Mentés and Andrea Locatelli for beamtime support, helpful discussions, and their critical reading of the manuscript; Matteo Lucian, and Wolfgang Neu for technical support; S. Savu, S. Abb and R. Kakavandi for cell calibration. Financial support from DFG under the contract CA852/5-1 is gratefully acknowledged. A.C. acknowledges Ente Cassa di Risparmio di Firenze, CeTeCS and EC through FP7-People-2011-IAPP (286196) ESN-STM.

## Notes and references

- 1 J. A. Venables, *Introduction to Surface and Thin Film Processes*, Cambridge University Press, 2000.
- 2 E. Bauer, *Z. Kristallogr.*, 1958, **110**, 372–394.
- 3 H. Brune, *Surf. Sci. Rep.*, 1998, **31**, 125–229.
- 4 Z. Zhang and M. G. Lagally, *Science*, 1997, **276**, 377–383.
- 5 A. Aviram and M. A. Ratner, *Chem. Phys. Lett.*, 1974, **29**, 277–283.
- 6 D. Gatteschi, A. Cornia, M. Mannini and R. Sessoli, *Inorg. Chem.*, 2009, **48**, 3408–3419.
- 7 M. Mas-Torrent, N. Crivillers, C. Rovira and J. Veciana, *Chem. Rev.*, 2011, **112**, 2506–2527.
- 8 R. Kakavandi, S.-A. Savu, L. Sorace, D. Rovai, M. Mannini and M. B. Casu, *J. Phys. Chem. C*, 2014, **118**, 8044–8049.
- 9 S. Abb, S.-A. Savu, A. Caneschi, T. Chassé and M. B. Casu, *ACS Appl. Mater. Interfaces*, 2013, **5**, 13006–13011.
- 10 R. Kakavandi, S.-A. Savu, A. Caneschi, T. Chasse and M. B. Casu, *Chem. Commun.*, 2013, **49**, 10103–10105.
- 11 R. Kakavandi, S.-A. Savu, A. Caneschi and M. B. Casu, *J. Phys. Chem. C*, 2013, **117**, 26675–26679.
- 12 A. Caneschi, D. Gatteschi, R. Sessoli and P. Rey, *Acc. Chem. Res.*, 1989, **22**, 392–398.
- 13 J. Choi, H. Lee, K.-j. Kim, B. Kim and S. Kim, *J. Phys. Chem. Lett.*, 2009, **1**, 505–509.
- 14 F. Grillo, V. Mugnaini, M. Oliveros, S. M. Francis, D. J. Choi, M. V. Rastei, L. Limot, C. Cepek, M. Pedio, S. T. Bromley, N. V. Richardson, J. P. Bucher and J. Veciana, *J. Phys. Chem. Lett.*, 2012, **3**, 1559–1564.
- 15 M. Souto, J. Guasch, V. Lloveras, P. Mayorga, J. T. López Navarrete, J. Casado, I. Ratera, C. Rovira, A. Painelli and J. Veciana, *J. Phys. Chem. Lett.*, 2013, **4**, 2721–2726.
- 16 S.-A. Savu, I. Biswas, L. Sorace, M. Mannini, D. Rovai, A. Caneschi, T. Chassé and M. B. Casu, *Chem. – Eur. J.*, 2013, **19**, 3445–3450.
- 17 F.-J. Meyer von Heringdorf, M. C. Reuter and R. M. Tromp, *Nature*, 2001, **412**, 517–520.
- 18 A. Locatelli, L. Aballe, T. O. Mentés, M. Kiskinova and E. Bauer, *Surf. Interface Anal.*, 2006, **38**, 1554–1557.



- 19 E. Bauer, *Rep. Prog. Phys.*, 1994, **57**, 895.
- 20 A. Locatelli and E. Bauer, *J. Phys.: Condens. Matter*, 2008, **20**, 093002.
- 21 H. Marchetto, U. Groh, T. Schmidt, R. Fink, H. J. Freund and E. Umbach, *Chem. Phys.*, 2006, **325**, 178–184.
- 22 S.-A. Savu, M. B. Casu, S. Schundelmeier, S. Abb, C. Tonshoff, H. F. Bettinger and T. Chassé, *RSC Adv.*, 2012, **2**, 5112–5118.
- 23 A. Scholl, Y. Zou, M. Jung, T. Schmidt, R. Fink and E. Umbach, *J. Chem. Phys.*, 2004, **121**, 10260–10267.
- 24 F. Tao and G. Q. Xu, *Acc. Chem. Res.*, 2004, **37**, 882–893.
- 25 J. Finster, E. D. Klinkenberg, J. Heeg and W. Braun, *Vacuum*, 1990, **41**, 1586–1589.
- 26 G. M. Ingo, N. Zacchetti, D. della Sala and C. Coluzza, *J. Vac. Sci. Technol., A*, 1989, **7**, 3048–3055.
- 27 A. Ermolieff, P. Bernard, S. Marthon and J. Camargo da Costa, *J. Appl. Phys.*, 1986, **60**, 3162–3166.
- 28 T. Suzuki, T. Lutz, D. Payer, N. Lin, S. L. Tait, G. Costantini and K. Kern, *Phys. Chem. Chem. Phys.*, 2009, **11**, 6498–6504.
- 29 M. L. M. Rocco, M. Haeming, D. R. Batchelor, R. Fink, A. Scholl and E. Umbach, *J. Chem. Phys.*, 2008, **129**, 074702.
- 30 M. B. Casu, B.-E. Schuster, I. Biswas, C. Raisch, H. Marchetto, T. Schmidt and T. Chassé, *Adv. Mater.*, 2010, **22**, 3740–3744.
- 31 M. Häming, A. Schöll, E. Umbach and F. Reinert, *Phys. Rev. B: Condens. Matter Mater. Phys.*, 2012, **85**, 235132.
- 32 E. F. Ullman, *J. Org. Chem.*, 1970, **35**, 3623–3631.
- 33 M. Fittipaldi, L. Sorace, A. L. Barra, C. Sangregorio, R. Sessoli and D. Gatteschi, *Phys. Chem. Chem. Phys.*, 2009, **11**, 6555–6568.

